Ecological Modelling 510 (2025) 111285

Contents lists available at ScienceDirect

Ecological Modelling

journal homepage: www.elsevier.com/locate/ecolmodel

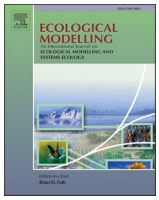

Integrating nitrogen and carbon cycling into LANDIS-II/PnET-Succession to improve forest landscape modeling: methods and sensitivity analyses

Zaixing Zhou [a,*], Eric J. Gustafson [b], Scott V. Ollinger [a], Andrew P. Ouimette [a,d], Brian R. Miranda [b,g], Matthew J. Duveneck [c,f], Jane R. Foster [e], Brian R. Sturtevant [b], Dustin R. Bronson [b], Danelle Laflower [f]

[a] Earth Systems Research Center, University of New Hampshire, Durham NH, USA
[b] USDA Forest Service, Northern Research Station, Institute for Applied Ecosystem Studies, Rhinelander WI, USA
[c] New England Conservatory, Boston MA, USA
[d] USDA Forest Service, Northern Research Station, Durham NH, USA
[e] USDA Forest Service, Southern Research Station, Knoxville TN, USA
[f] Harvard Forest, Harvard University, Petersham, MA, USA
[g] USDA Forest Service, Eastern Planning Service Group, La Crosse WI, USA

ARTICLE INFO

Keywords:
LANDIS-II
PnET-CN
PnET-Succession
Landscape modeling
Nitrogen cycling
Carbon cycling

ABSTRACT

Carbon (C) and nitrogen (N) cycles are closely coupled in forested ecosystems. Studies of interactions between nitrogen cycling and forest succession have been challenging due to the broad spatial and temporal scales involved in feedbacks between successional dynamics and N cycling mechanisms. In this study, algorithms were added to a forest landscape model (LANDIS-II/PnET-Succession extension) to account for nitrogen cycling and its effects on growth and competition. In the revised model, PnET-CN-Succession, with coupled C and N cycling, forest species compete for not only light and water resources, but also for nutrients. Parameterized and validated for both deciduous and evergreen (hemlock) stands at Harvard Forest, Massachusetts, USA, along with a sensitivity analysis, the PnET-CN-Succession model replicated empirical C and N cycling patterns in deciduous and coniferous forests under a N constraint. Predicted C and N cycles were faster in deciduous forests, but more tightly coupled in evergreen forests. Analysis of harvesting scenarios demonstrated that N constraints reduced rates of biomass accumulation in early to mid-successional stages, compared to results from simulations with a version of PnET-Succession that did not simulate N cycling. Predicted changes in post-harvest species composition agreed with the observed successional patterns at Harvard Forest. By accounting for an important constraint on tree growth and competition, PnET-CN-Succession is a valuable tool to improve our ability to predict forest dynamics in response to various scenarios of forest management and global changes.

1. Introduction

The dynamics of forest composition, biomass accumulation, and their spatial patterns are driven by disturbance, reproduction, growth, competition, and death of individual trees (Payne and Peet, 2023), which collectively form a shifting mosaic of ecological communities through time and space. The aim of forest landscape models is to integrate these successional processes and connect them with interacting disturbances and global change through time and a broad spatial scale (10^4–10^8 ha) to simulate forest dynamics (Larocque et al., 2016).

In recent decades, there has been growing interest in incorporating more mechanistic plant physiology along with influential biogeochemical and hydrological features into forest succession models (Gustafson, 2013; Huston, 1991; Scheller, 2018), especially for studies of novel environmental conditions, such as climate change (Gustafson et al., 2020) or invasive pathogens/pests (Gustafson et al., 2022). For example, the LANDIS forest landscape model has evolved through gradual additions of mechanisms affecting succession and disturbance interactions (e.g., Sturtevant et al., 2004). Scheller and Mladenoff (2004) initially supplemented the standard LANDIS model cohort (a group of trees of the same species based on their ages) 'currency' from age (Mladenoff, 2004) to include cohort biomass, and then loosely coupled LANDIS to an

* Corresponding author.
E-mail address: zaixing.zhou@unh.edu (Z. Zhou).

https://doi.org/10.1016/j.ecolmodel.2025.111285
Received 20 October 2024; Received in revised form 10 July 2025; Accepted 31 July 2025
Available online 8 August 2025

ecosystem model (PnET-II) (Aber and Federer, 1992; Xu et al., 2009) to produce a biomass succession extension within the LANDIS-II forest landscape model (Scheller et al., 2007). de Bruijn et al. (2014) took a further step by fully integrating PnET-II algorithms into a LANDIS-II succession extension to explicitly simulate the competition of tree species cohorts for light and water on each landscape cell at a monthly time-step (i.e., PnET-Succession). These models can be coupled with disturbance modules such as fire, wind, and timber harvest.

Growth and competition in forest landscape models are often regulated by energy, carbon (C) and water cycling (or proxies thereof, i.e., growing space) and few such models account for nutrient constraints, e.g., LANDIS-II NECN (Scheller et al., 2011). Because C and N cycling are closely coupled in terrestrial ecosystems, N availability is significantly correlated with photosynthesis and growth at scales ranging from leaf (Wright et al., 2004) to canopy (Ollinger et al., 2008) to ecosystem (Ollinger and Smith, 2005). When limited nitrogen resources are available, the competition for nitrogen can become a significant constraint on the growth of species, potentially impacting successional outcomes. This importance of C and N coupling can be exacerbated by timber harvesting or global environmental change, e.g., an increase in atmospheric N deposition (Bobbink et al., 2010) and an increase in atmospheric CO_2 (Mason et al., 2022). Consequently, it is becoming increasingly apparent that nitrogen cycling should be incorporated into forest landscape models to make their projections more accurate (Scheller, 2018).

There has also long been interest in the effect of forest succession and species assemblages on patterns of nitrogen cycling through time (Crowley et al., 2016). Nitrogen cycling exhibits specific patterns (e.g., rates of soil mineralization, plant N uptake, and stream N export dynamics) at various stages of forest succession (Dybzinski et al., 2013; Goodale and Aber, 2001; Vitousek et al., 1989), which can be related to successional stages and forest functions (Vitousek and Reiners, 1975). For example, Lovett et al. (2018) showed that N retention increased in the Hubbard Brook Experimental Forest (New Hampshire, USA), even in late succession stages. Emerging questions, such as the causes of N oligotrophication (Groffman et al., 2018) and the global decline in foliar nutritional status (Penuelas et al., 2020; Mason et al. 2022), require methods to fully examine the interaction between N cycling and forest succession in a changing environment.

In this study, we modified a commonly used forest landscape model (the PnET-Succession extension of LANDIS-II, Gustafson et al., 2023) to account for nitrogen cycling and its effect on growth and competition to improve simulated successional dynamics in response to disturbance and climate change. This type of landscape succession model can be valuable to address the interactions between forest succession and nutrient constraints. Specifically, we incorporated algorithms of nitrogen and its associated carbon cycling from PnET-CN (Aber and Driscoll, 1997) into PnET-Succession, enabling the simulation of nitrogen and carbon dynamics and accounting for their constraints on growth and competition. Our objectives were to 1) integrate the N and C cycling algorithms of PnET-CN into PnET-Succession, 2) validate the revised model at the grid-cell scale, 3) conduct a sensitivity analysis of the nitrogen parameters and algorithms on forest growth, and 4) demonstrate the effect of model revisions on projected forest dynamics using various harvesting scenarios.

2. Methods

2.1. LANDIS-II/PnET-Succession model

The LANDIS-II forest landscape model (Scheller et al. 2007) simulates the successional response of forests to disturbances at the landscape scale (10^4 – 10^8 ha). PnET-Succession is one of several optional succession extensions to LANDIS-II, and it is among the more mechanistic succession extensions available. The PnET-Succession Extension expands on LANDIS-II Biomass Succession Extension with several key advances. For example, rather than simulating growth using a fixed species maximum growth rate (estimated *a priori* by the PnET-II model for specific combinations of soils and climate) and species interactions as competition of cohorts within an abstract growing space, PnET-Succession uses the algorithms of PnET-II to dynamically simulate growth of each cohort as affected by competition for available light and water. Ecophysiological parameters of species cause cohorts to be differentially stressed by abiotic conditions, resulting in successional dynamics that are further influenced by life history attributes affecting seed-dispersal, establishment, growth, competition, and disturbances. Leaf area index (LAI) is tracked as an additional tree species cohort attribute, such that competition for light in both vertical and horizontal dimensionsis explicitly simulated (Gustafson et al., 2024), while soil water balance is simulated at the cell scale to simulate cohort stress from either too little or too much water (Gustafson et al. 2023).

The above capabilities are derived from PnET (Photosynthesis and EvapoTranspiration), a simple, lumped parameter model of carbon and water balances of forest stands (Aber et al., 1995), which was initially built on two principal relationships: 1) maximum photosynthetic rate (Amax) is a function of foliar nitrogen concentration (g leaf N/g leaf dry biomass), and 2) evapotranspiration is a function of the realized photosynthetic rate, modified by a water use efficiency parameter and atmospheric vapor pressure deficit. PnET-Succession specifically uses the photosynthesis and respiration equations from PnET-II to simulate photosynthesis in stacked canopy sublayers and allocation of photosynthates to specific cohort biomass components (root, foliage, wood, and non-structural carbon). Various stressors, respiration costs, and biomass turnover (chronic loss from biomass pools) are simulated as a reduction factor applied to optimal photosynthesis rates. The user-defined time step of PnET-Succession controls the frequency of outputs and the timing of its interaction with other extensions, while the internal time step of PnET-Succession is always monthly. This allows simulated cohorts to respond to biotic and abiotic conditions on a monthly basis, producing greater responsiveness to changing climatic and atmospheric conditions as well as more extreme events.

2.2. Nitrogen and carbon processes newly integrated

The PnET-CN model (Aber and Driscoll, 1997) is a variant of PnET-II that adds decomposition and N cycling mechanisms, resulting in fully coupled cycles of carbon, nitrogen and water. N cycling mechanisms simulated include nitrogen mineralization through soil organic matter decomposition, microbial N immobilization, plant nitrogen uptake, nitrification, and nitrate leaching. In PnET-II, the foliar N concentration for each species remains fixed at a user-prescribed value, but in PnET-CN, foliar N is dynamic and is driven by interactions between plant N demand and soil N supply (Aber and Driscoll, 1997). A simple soil carbon cycling routine integrated with the soil N cycling routine also enables full carbon accounting (including soil C). Here, we describe a new LANDIS-II succession extension (PnET-CN-Succession) that incorporates nitrogen and carbon cycling algorithms from PnET-CN (Fig. 1) to enable successional dynamics to respond to nutrient abundance and improved carbon accounting.

At different spatial scales, carbon and nitrogen cycles interact in compartments of live biomass (foliage, live wood, and fine roots), litter (foliage, dead wood, and fine roots), and soil organic matter in the PnET-CN-Succession model. Within cohorts, the dynamic of foliar N concentration depends on the relative availability of C and N to plants. An internally calculated nitrogen limitation variable, NRatio (Eq. (1)), is computed annually based on the internal N pool within cohorts (PlantN). When the PlantN pool is high (high NRatio, low N stress), N concentration in foliage, wood, and root increases. A large PlantN pool also reduces the efficiency of N uptake (RootNSinkEff, Eq. (2)) from available pools of ammonium (NH_4^+), and nitrate (NO_3^-). This increase in foliar N results in increased net photosynthesis and increases the cohort carbon pool (PlantC), NPP, and biomass accumulation. This increased

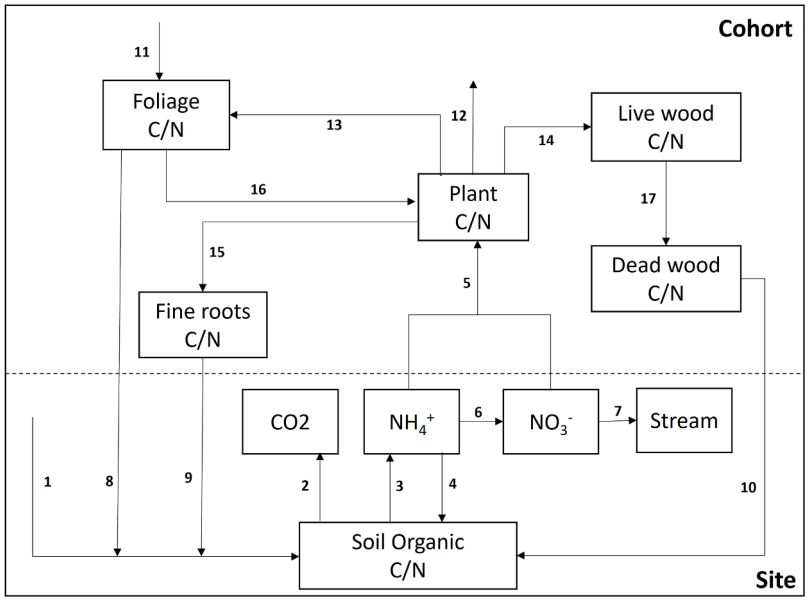

Fig. 1. Structure of C and N pools and processes associated with C/N cycling in PnET-CN-Succession. Boxes represent pools, numbered arrows represent fluxes, and the dotted horizontal line separates the cohort and site scale: (1) N deposition (2) Soil organic matter (SOM) decomposition (3) N mineralization (4) N immobilization (5) Plant N uptake (6) Nitrification (7) N leaching (8) Foliar litterfall (9) Root litter (10) Wood decay (11) Photosynthesis (12) Growth and maintenance respiration (13) Allocation to leaves (14) Allocation to wood (15) Allocation to roots (16) Foliage N retranslocation before senescence (17) Wood turnover and litter. Pools and processes are tracked at two scales, i.e. per cohort and per site. There can be one to many cohorts on any single site (cell) (Gustafson et al. 2023). Each cohort on a site has its own C and N pools, and cohorts contribute to and compete for the soil (site) C and N pools.

NPP requires additional N from PlantN to produce biomass according to its stoichiometric C:N ratio, which decreases the PlantN pool. At the cell scale, all cohorts contribute to the soil organic pool (foliar litter, dead root, and dead wood). High C:N ratios in litter decrease soil net N mineralization (the difference between gross N mineralization and microbial N immobilization), therefore reducing NH_4^+ availability. Soil NH_4^+ can be nitrified to NO_3^- that can leach out of the soil matrix and become unavailable to cohorts. The rate of nitrification is a function of cohort competition for N. When a cohort is N stressed (i.e., low NRatio), the nitrification rate decreases due to the increasing strength of cohort demand for N (high RootNSinkEff). Consequently, NO_3^- decreases along with NH_4^+, and more N is preserved in the soil for potential cohort uptake, reducing cohort N stress and promoting increased foliar N concentration. A more complete description of these PnET-CN carbon and nitrogen cycling equations can be found in (Aber et al., 1997).

$$NRatio = 1 + \frac{PlantN}{MaxNStore} * FolNConRange \quad (1)$$

$$RootNSinkEff = \sqrt{1 - \frac{PlantN}{MaxNStore}} \quad (2)$$

where MaxNStore is the maximum cohort PlantN pool and FolNconRange represents a potential range of foliage nitrogen concentration for each species that are defined by users in the input.

2.3. Nitrogen competition among cohorts

Because LANDIS-II allows multiple cohorts to occur on the same grid cell, several new algorithms were needed to simulate competition for nitrogen among cohorts. The first computes a cell-level average N uptake potential across all cohorts (RootNSinkEffavg; Eq. (3)) by weighting each cohort's N uptake potential according to its relative biomass, $\frac{x}{\sum x}$. From this cell- level average N uptake potential and concentrations of available N in soil, a total cell-level nitrogen uptake from the soil is then calculated (Eq. (4)). Nitrogen uptake is distributed among cohorts by multiplying the relative cohort nitrogen uptake strength, $\frac{RootNSinkEff * \frac{x}{\sum x}}{RootNSinkEffavg}$ and the total N uptake at the cell (Eq. (5)). These new algorithms allow for the N uptake of individual cohorts to be regulated by total cell-level N availability, as well as relative biomass and N stress (or N demand) of each cohort.

$$RootNSinkEffavg = \sum \left(RootNSinkEff * \frac{x}{\sum x} \right) \quad (3)$$

$$PlantNUptakeSite = RootNSinkEff * \left(NH_4^+ + NO_3^- \right) \quad (4)$$

$$PlantNUptakeCohort = PlantNUptakeSite * \frac{RootNSinkEff * \frac{x}{\sum x}}{RootNSinkEffavg} \quad (5)$$

2.4. Study site

We tested the model by conducting simulations at the Harvard Forest (HF) in central Massachusetts, USA where much previous research with PnET and LANDIS has been conducted (Duveneck et al., 2017; Zhou et al., 2018). We focused on a deciduous hardwood stand (EMS) and an evergreen hemlock stand (HEM) at HF where data for C and N fluxes as well as forest community composition were available for model parameterization and validation.

The climate at HF is cool and moist with July mean temperature 20 °C, January mean temperature −7 °C, and annual mean precipitation 110 cm, distributed evenly throughout the year. The soils are mainly sandy loam glacial, with some alluvial and colluvial deposits, and moderately to well-drained in most areas (Foster, 1992). Harvard Forest is predominantly covered by a temperate mixed forest representing the transition hardwood-white pine (*Pinus strobus*)-eastern hemlock (*Tsuga canadensis*) vegetation zone of central New England. Deciduous species are primarily Northern red oak (*Quercus rubra*), red maple (*Acer rubrum*), and black birch (*Betula lenta*). Red pine (*Pinus resinosa*) and Norway spruce (*Picea abies*) are also present (Foster, 1992). The study area has been subjected to a complex array of historic agricultural and logging treatments as well as natural disturbances (Foster, 1992).

The environmental measurement station (EMS) eddy flux tower

(42.5378 °N, 72.1715 °W) located on the Prospect Hill tract of Harvard Forest has a record of eddy covariance CO_2 exchange measurements that began in 1991 (Munger and Wofsy, 2024a). The area surrounding the tower is dominated by red oak and red maple, with scattered eastern hemlock and white pine. The stand is approximately 85–120 years old, having been established on abandoned farmland. A second flux tower (42.5393 °N, 72.1779 °W), the hemlock flux tower (HEM), is also located on the Prospect Hill tract in a mesic hemlock-dominated forest with most trees 100–200 years old on undisturbed soils. Other tree species present include red maple, black birch, red oak, and white pine. The hemlock woolly adelgid (*Adelges tsugae,* HWA) was detected at HEM since 2009 (Ellison et al., 2018).

2.5. Model application and validation

We ran the model at the EMS and HEM sites separately using the cell mode which considered a landscape as one simple area with the same initial conditions of soil, climate, and nutrients. Specifically, we treated respectively the EMS site or HEM site as a 7 × 7 gridded landscape consisting of 100 m × 100 m cells. All cells within a site (i.e., EMS or HEM) were initialized with the same starting conditions of soil, climate, nutrients, and initial cohorts. However, different sites had different starting conditions. Multiple species and cohorts, defined by the initial communities in the model input, coexisted on each cell, competing for space and resources. That treatment didn't represent the real landscape around the site. It facilitated the model application by producing 49 replicates for each site simulation and allowed us to account for stochastic effects that can cause neighboring cells to deviate over time, e.g., via seed dispersal and new cohort establishments. Aggregated results were then used for validation and comparison.

The simulation at the EMS site started in year 1991, based on forest community composition in that year, as reported by Barford et al. (2001). The simulated community included an oldest cohort of 97-year--old red oak and a youngest of 52- year-old red oak. Modeling parameters relevant to the PnET-Succession were from Duveneck et al. (2017), and modeling parameters relevant to the N cycling were from Zhou et al. (2018) and Ollinger et al. (2002a). A selected list of species parameters at both EMS and HEM can be accessed on the GitHub (https://github.com/zaixingzhou/PnET-CN-Succession/blob/main/EcologicalModeling_2024/ModelingParameters-SPECIES.xlsx). Detailed conceptual models, parameters, inputs, and outputs can be accessed in the PnET-Succession v5.1 User Guide (https://github.com/zaixingzhou/PnET-CN-Succession/blob/main/LANDIS-II%20PnET-Succession%20v5.1 %20User%20Guide.docx). We compared modeled results with field data at the EMS site, including eddy covariance estimates of gross primary production (GPP) and net ecosystem production (NEP); above-ground biomass (AGB); and leaf area index (LAI); and canopy N concentration (Munger and Wofsy, 2024b). Eddy covariance measurements of C and water fluxes at the HEM tower started in the summer of 2004 (Foster and Barker Plotkin, 2023). The HEM simulation started in year 1991 with a forest community composition of a 100-year-old hemlock cohort and a-230-year old hemlock cohort, whose age data were estimated from Hadley and Schedlbaurer (2002). Field data at HEM, such as GPP, NEP, above-ground biomass, canopy N concentration, and LAI (Orwig and Hadley, 2024) were also compared with modeled results.

Stream N exports from Arthur Brook upper pipe watershed (AU) at Harvard Forest (Fulweiler and Orwig, 2024) were used for comparison with modeled mineral N export in this study. AU represents an upland headwater watershed of 24 ha, which consists of approximately 60 % evergreen trees, including hemlock and white pine, and 40 % deciduous trees, primarily red oak and red maple. The EMS and HEM sites are located approximately 500–700 m south, outside of the watershed. We didn't conduct separate simulations for the watershed itself as we didn't have the spatially distributed forest composition in the watershed. Nonetheless, we felt that the measured steam N exports as a reference could still be useful given the close proximity and general similarities in forest conditions.

PnET-CN-Succession requires atmospheric nitrogen deposition rate (NDep, gN m^{-2} $month^{-1}$) as an input. Measured total wet N deposition measurements were collected near the Quabbin Reservoir, 17 km southwest of the Harvard Forest (NADP, 2019), and was linearly extrapolated back to pre-industrial background levels using data from Galloway et al. (2004).

2.6. Sensitivity analysis of the N cycling parameters/input

We conducted a sensitivity analysis of parameters/input that influence N cycling by varying the value of relevant parameters/input by ± 25 % to assess their impacts on aboveground biomass (AGB). The parameters varied were N deposition rate (NDep, input from the climate file), decomposition rate (Decom, 0.075 yr^{-1}), minimum foliar N in leaf litter (FLPctN, varying with species), and Foliar N variability constant (FolNRng, 0.6). NDep specifies exogenous nitrogen inputs that vary annually. Decom determines the relative N mineralization rate, with higher values producing more mineral nitrogen in the soil available for plants. FLPctN represents the lowest limit of foliar N concentration observed in cohorts of a species, and FolNRng constrains how high foliar N can get given unlimited N availability. In general, to prioritize foliar mass and photosynthesis, trees optimize nutrient allocations to conserve foliar N ecophysiologically, as a growth strategy. Simulated results were aggregated for the most recent 30 years at both EMS and HEM sites.

2.7. Timber harvest scenario analysis

We conducted a timber harvesting simulation experiment to assess how accounting for C and N cycling affected predicted successional outcomes. We simulated three different levels of above-ground biomass removal (30 %, 60 %, and 100 %) from each site with the universal dispersal algorithm, thus resetting succession differently. The EMS site was used for this experiment and harvesting was implemented in the year 2020. To isolate the effects of harvesting, we held the future physical and chemical climate fixed, with a CO_2 concentration of 412 ppm and N deposition of 3.6 kg N ha^{-1} yr^{-1}. All parameters other than those we varied experimentally were also held constant. As a comparison, growth and competition were simulated for 400 years with and without the influence of N cycling using PnET-Succession v5.1 (no CN dynamics simulated) and PnET-CN-Succession v1.0 (CN dynamics simulated). These two model versions were identical other than the CN algorithms described above. Successional outcomes were quantified using species' relative abundance based on aboveground biomass (AGB) composition and total AGB at the timestep prior to cutting, 20 years after harvesting (early succession stage), 120 years after harvesting (mid-succession stage), and 250 years after harvesting (late succession stage). Species were grouped into three categories (Uchytil, 1991), early succession species (pioneers), including paper birch (*Betula papyrifera*), large-tooth aspen (*Populus grandidentata*), and pin cherry (*Prunus pensylvanica)*, mid-succession species, including red maple, red oak, and yellow birch (*Betula alleghaniensis*), and late succession species, including eastern hemlock, sugar maple (*Acer saccharum*), American beech (*Fagus grandifolia*), red spruce (*Picea rubens*).

3. Results

3.1. Validation of carbon cycling

In the deciduous stand (EMS), the PnET-CN-Succession modeled monthly GPP showed similar seasonal dynamic patterns with the tower data although the model underestimated the GPP during the summer from 2001 to 2013 (Fig. 2a). The r^2 of predicted versus observed monthly values during the growing season at EMS was 0.85 ($p < 0.001$), with the average annual values of tower GPP of 1504.2 ± 214.3 g C m^{-2} $year^{-1}$ and modeled GPP of 1519.2 ± 165.0 g C m^{-2} $year^{-1}$. Although

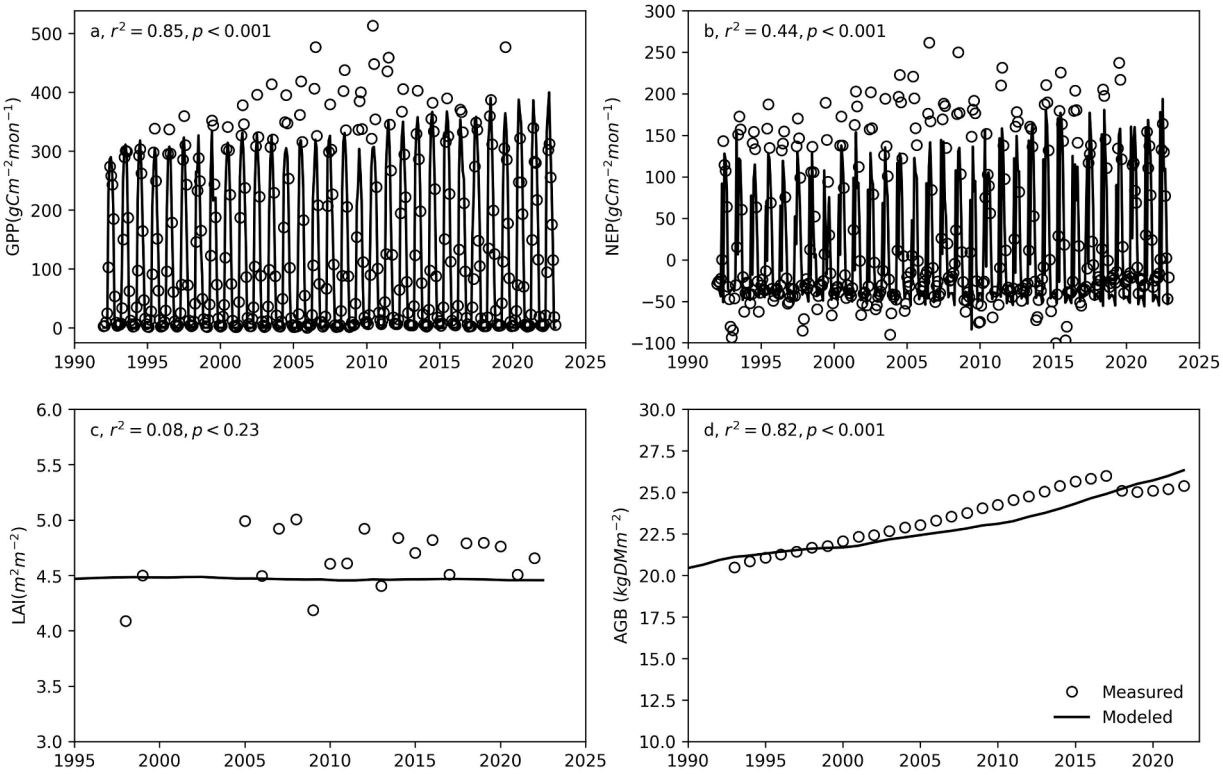

Fig. 2. Predicted a) GPP, b) NEP, c) LAI, and d) AGB in the deciduous stand compared to observed data from EMS site. The dots are measured data while the black line is modeled. The r^2 and p-value are statistical indicators derived from the linear regression between predicted and observed values.

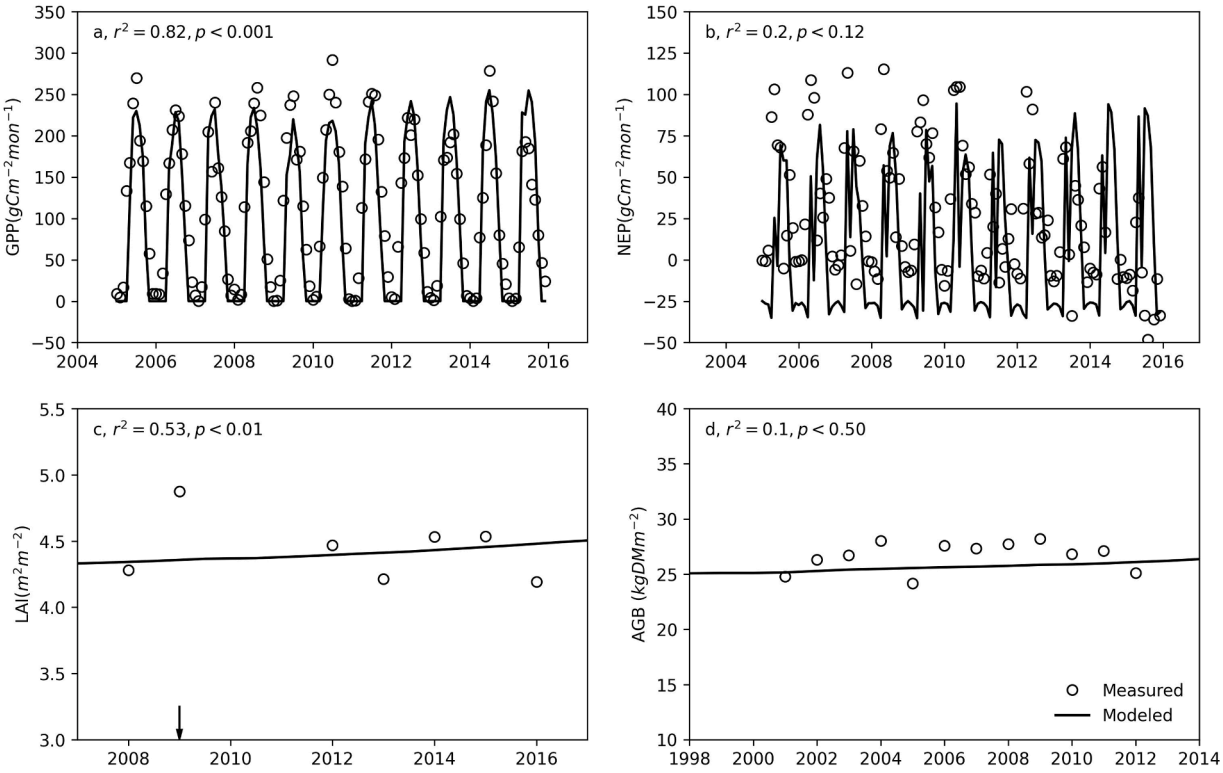

Fig. 3. Predicted a) GPP, b) NEP, c) LAI, and d) AGB in the hemlock stand compared to observed data from HEM site. The arrow in panel c indicates the year (2009) in which the hemlock woolly adelgid infestation was first observed in the stand. The r^2 and p-value are statistical indicators derived from the linear regression between predicted and observed values.

patterns of NEP were similar to those for GPP, the r^2 of predicted versus observed monthly values were only 0.44 ($p < 0.001$). On average, the model underestimated the annual NEP by 58 % (127.8 ± 72.9 g C m^{-2} yr^{-1} vs 311.4 ± 151.8 g C m^{-2} yr^{-1}), mostly due to the underestimated GPP from 2001 to 2013. The predicted mean LAI (4.47 ± 0.01) was consistent with the measurements (4.65±0.25, Fig. 2c). Predicted values for annual above-ground biomass were also consistent with the observations with a r^2 of 0.82 ($p < 0.001$). Due to a mortality event (not simulated in the modeling), the observed biomass dropped in 2018.

The r^2 of predicted monthly GPP versus observed values at the HEM site was 0.82 ($p < 0.001$), with average annual values of observed GPP of 1330.8 ± 169.1 g C m^{-2} $year^{-1}$ and modeled GPP of 1091.5 ± 80.8 g C m^{-2} $year^{-1}$ (Fig. 3a). However, the predicted monthly NEP patterns were not consistent with observed patterns (Fig. 3b; r^2=0.2, $p < 0.12$). In 2009, the hemlock stand was infested by hemlock woolly adelgid (Ellison et al., 2018), which caused the stand to be gradually degraded as a C sink. Overall, the correlation between predicted and observed yearly NEP has a r^2 of 0.32 ($p < 0.07$). Although the adelgid infested 98 % of hemlock trees by 2015 (Foster and Barker Plotkin, 2023), the forest canopy was not noticeably thinning until after 2019 with a reduced LAI (data not shown). On average, the predicted annual LAI during 2008–2016 (4.5 ± 0.1) was in line with the observed data (4.3 ± 0.3) (Fig. 3c). The predicted values of annual above-ground biomass (25.6 ± 0.28 kg dry matter/m^2) fell in the range of the observations (26.6 ± 1.3 kg dry matter/m^2).

3.2. Validation of nitrogen cycling

At the EMS site the predicted canopy N % (aggregated species N content weighted by cohort leaf biomass) were consistent with observed values before the year 2011 ($p < 0.01$) but were overestimated afterward (Fig. 4a), due to a decline in measured %N that model predictions didn't replicate. Overall, the predicted canopy N % had a slightly increasing tendency after the year 1995 ($p < 0.01$). The cause of the decrease in canopy N % at EMS in recent years is still elusive. Recent studies (Groffman et al., 2018; Penuelas et al., 2020) demonstrated that the decrease in hardwood forest foliar N concentrations was well correlated with the increasing atmospheric CO_2 concentration. However, the predicted canopy N %, which included the effect of the rising CO_2 concentration on leaf photosynthesis didn't capture this trend. In the hemlock stands, there was less variability in predicted canopy N % (1.13 ± 0.01) which was in agreement with the measured data (1.20 ± 0.11) on average.

The observed (0.01± 0.002 gN m^{-2} yr^{-1}) and simulated N exports in both deciduous (0.09± 0.03 gN m^{-2} yr^{-1}) and hemlock stands (0.03± 0.01 gN m^{-2} yr^{-1}) were less than the input N deposition (Fig. 4b), suggesting both stands are still accumulating N (Figs. 2d and 3d). Compared to the observed stream N export at Arthur upper pipe gauge, modeled N exports in both stands were overestimated. Moreover, the predicted N export in the deciduous stand was much greater than that in the hemlock stand, suggesting a faster nitrogen cycling in the deciduous stand, which also had a greater canopy N content (Fig. 4a).

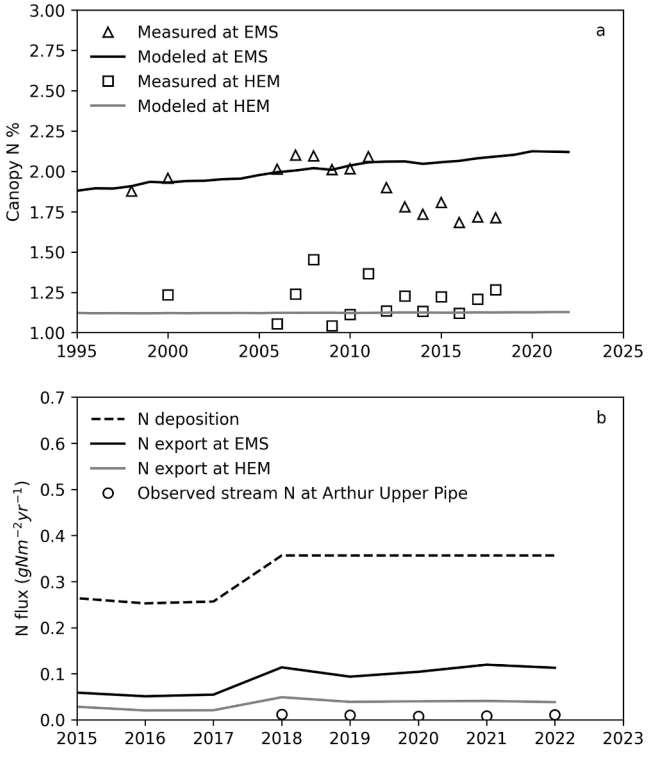

Fig. 4. Predicted a) canopy N % and b) N export in the deciduous stand (EMS) and the hemlock stand (HEM) compared to observed stream N export at the Arthur upper pipe gauge. The symbols represent observed data. The solid black line represents modeled results in the deciduous stand and the solid gray line in the hemlock stand. $r^2 = 0.19$ and $p < 0.11$ were derived from the linear regression between predicted and observed N % for all observed years at the EMS site, while $r^2 = 0.01$ and $p < 0.83$ at the HEM site.

3.3. Sensitivity analysis

In the sensitivity analysis, foliar N concentration (FLPctN) was found to be the most sensitive N cycling parameter, for both deciduous and coniferous biomass growth (Fig. 5). These results are consistent with findings that foliar N is generally the most important physiological trait for photosynthesis (Wright et al., 2004; Zhou et al., 2018). Our analyses demonstrated slightly different responses to changes in N cycling between deciduous and coniferous forests. Larger variations in AGB response were found in deciduous species (EMS) than in the hemlock stand (Fig. 5). In the deciduous EMS site, elevated N cycling parameter values (increased N deposition (NDep+25 %), decomposition rate (Decom+25 %), foliar N content (FLPctN+25 %), and maximum foliar N (controlled by FolNRng)) promoted biomass growth and accumulation, reflecting a fast plant-soil feedback (Ollinger, 2003). Conversely, AGB at the hemlock site did not show strong responses to parameter changes,

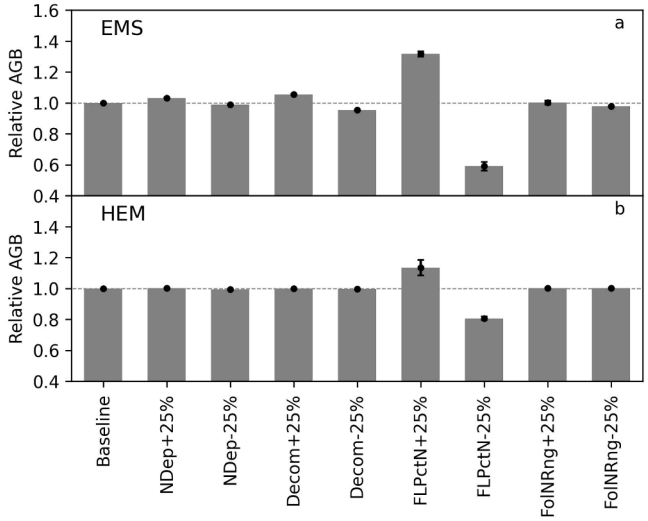

Fig. 5. Sensitivity of site above-ground biomass (AGB) to variation of key N cycling parameters in the deciduous stand (EMS) and the evergreen hemlock stand (HEM). Baseline simulations used the same input and parameters used for validation. Selected parameters were varied by ±25 % as indicated in x-axis labels. The dashed line serves as a reference (Baseline). The y-axis presents AGB values relative to the results of the baseline.

except for foliar N concentration (FLPctN), even when N deposition varied (NDep).

3.4. Scenario analysis

The timber harvesting scenario analysis comparing results from PnET-Succession and PnET-CN-Succession showed consistent patterns in the dynamics of forest composition (Figs. 6, 7, A1 and A2) when forests were allowed to grow long enough to reach the late-successional stage. AGB generally reached its maximum in about 100 years (Figs. 6, A1, and A2), but forest species composition transitioned with succession (Figs. 7b-d, A1 and A2) in ways that were consistent with field observations of successional changes in the northern hardwood forests of New Hampshire, USA (Leak, 1991). e.g., following clearing (100 % harvest), during the early stage of regrowth phase (20 years after cutting), the forest was dominated by early successional species, such as aspen and paper birch. During the mid succession stage (120 years after cutting), mid successional species (e.g., red maple, red oak, and white pine) dominated the forest plus a significant amount of late successional species (e.g., beech, hemlock, and sugar maple). In the late stage (250 years after cutting), the forest was dominated by late successional species (e.g., beech, hemlock, sugar maple, and yellow birch) supplemented by mid successional species (e.g., red oak and white pine). The simulated maximum AGB was also in the range of the FIA (USDA Forest Service Forest Inventory and Analysis) estimates, 23.9 ± 7.5 (kg DM m^{-2}), for the region around Harvard Forest (Finzi et al., 2020).

The nitrogen cycling processes in the model, i.e., PnET-CN-Succession, didn't alter the dynamics of species abundance throughout succession, in terms of grouped species, after harvesting disturbance, compared to PnET-Succession (Fig. 7). Instead, it mainly impacted the biomass dynamics by limiting the nitrogen nutrient and carbon assimilation. At the early to mid stage of succession (2020–2200), the biomass simulated by PnET-CN-Succession was less than that simulated by PnET-Succession ($p < 0.001$) because nutrient constraints (e.g., net mineralization, Fig. 6) led to a lower canopy N, on average, 1.76 % compared to 1.85 % by PnET-Succession. However, since the forest simulated by PnET-CN-Succession kept sequestrating nitrogen from atmospheric deposition (about 200 years), it would lead to a similar carbon status at the late-succession stage as simulated with PnET-Succession (Fig. 6). Gaps opened by harvesting or mortality mainly drove the species regeneration and establishment in the models and thus composition dynamics (Gustafson et al., 2023), and nitrogen cycling in PnET-CN-Succession modified cohort growth rates in this case study.

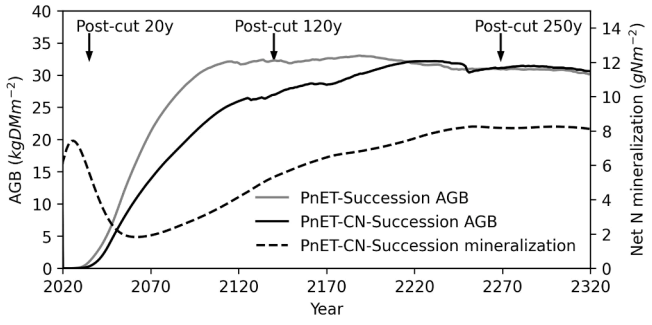

Fig. 6. Comparison of site above-ground biomass (AGB) after harvesting in the 100 % harvesting scenario between the two models. Harvesting was prescribed in the year 2020. The arrows mark the early (20 years after cutting), mid (120 years after cutting), and late (250 years after cutting) succession stages along the dynamics of AGB. Species compositions at each stage are shown in Fig. 7. From 2020–2200, AGB simulated by PnET-CN-Succession was significantly lower than that simulated by PnET-Succession ($p < 0.001$), based on a repeated measures ANOVA test.

4. Discussion

4.1. Importance of canopy N

The impact of adding N cycle to this succession model is primarily driven by the fundamental relationship of photosynthetic capacity to foliar nitrogen in leaves (Wright et al., 2004). Our sensitivity analysis showed that foliar N was the most sensitive nitrogen cycling factor in our model for simulating AGB (Fig. 5), consistent with other studies (Ollinger and Smith, 2005). An accurate estimate of foliar N dynamic in the simulation can greatly improve forest growth. In the prior version of the model, PnET-Succession, foliar N is prescribed as a fixed input species parameter that doesn't vary through the simulation. This ignores the impacts of disturbance and N deposition on N cycling, either of which typically leads to a varying foliar N (Ollinger et al., 2002b). Furthermore, a fixed foliar N cannot reflect cohort competition for N. One of the major goals in this study for integrating nitrogen cycling processes into PnET-Succession is to produce a dynamic foliar N based on plant-soil N cycling feedbacks. In our validation testing of these new capabilities, good agreement between predicted and observed canopy N (Fig. 4) generated predictions of GPP and LAI, and thus AGB biomass (Figs. 2 and 3) that were consistent with observations, but less consistent predictions of NEP due to poor estimation of ecosystem respiration.

4.2. Species difference

Deciduous and coniferous forests generally show different patterns of carbon and N cycling in field studies (Augusto et al., 2015). In our study, the deciduous site (EMS) demonstrated a faster C and N cycling than the coniferous site (HEM), including larger observed GPP, NEP (Fig. 2), canopy N, modeled nitrogen leaching (Fig. 4), modeled mineralization and nitrification rates (not shown here). We also observed greater variations in foliar N in deciduous forests (Fig. 4a). The deciduous stand was more sensitive to parameter settings in the sensitivity analysis. Ollinger et al., (2002b) showed that deciduous species can respond more to changing soil N availability, both through within-species variation, and through shifting species composition. In contrast, hemlock forests demonstrated a tighter C and N coupling, which were not very responsive to changes in the N cycling factors shown in the sensitivity analysis. Lower leaf nutrient concentration led to reduced carbon assimilation (Fig. 3) and decomposition that resulted in low inorganic nitrogen leaching (Fig. 4).

Given the distinct carbon and nitrogen cycling patterns of different species, a shift of forest structure and composition in the landscape (e.g., resulting from selected harvesting or invasive pest mortality), is expected to have significant impacts on ecosystem functions and services (Ford et al., 2012; Orwig et al., 2013). Since hemlock woolly adelgid started infesting hemlock trees at HEM in 2009, the hemlock stand has been declining, resulting in reduced GPP, LAI, and NEP (Fig. 3). Hardwood deciduous species, including black birch (*Betula lenta*), red maple, and red oak species, are becoming established in the canopy gaps resulting from hemlock mortality (Ford et al., 2012). Studies have reported that adelgid-induced canopy thinning and tree mortality can lead to significantly accelerated decomposition, enhanced nutrient cycling rates, increased nutrient availability, and thus increased nitrogen leaching to streams (Cessna and Nielsen, 2012; Jenkins et al., 1999). A model, such as PnET-CN-Succession, with coupled carbon and N cycling, would be valuable to address the impacts of such invasive pests on the hemlock forests (Crowley et al., 2016) by being parameterized to have pest mortality in the simulation.

4.3. Sources of uncertainty

In this study, the revised model demonstrated its new basic functions for exploring patterns of N cycling dynamics through successional stages (e.g., Fig. 4) as well as nitrogen feedback to forest productivity (Fig. 5)

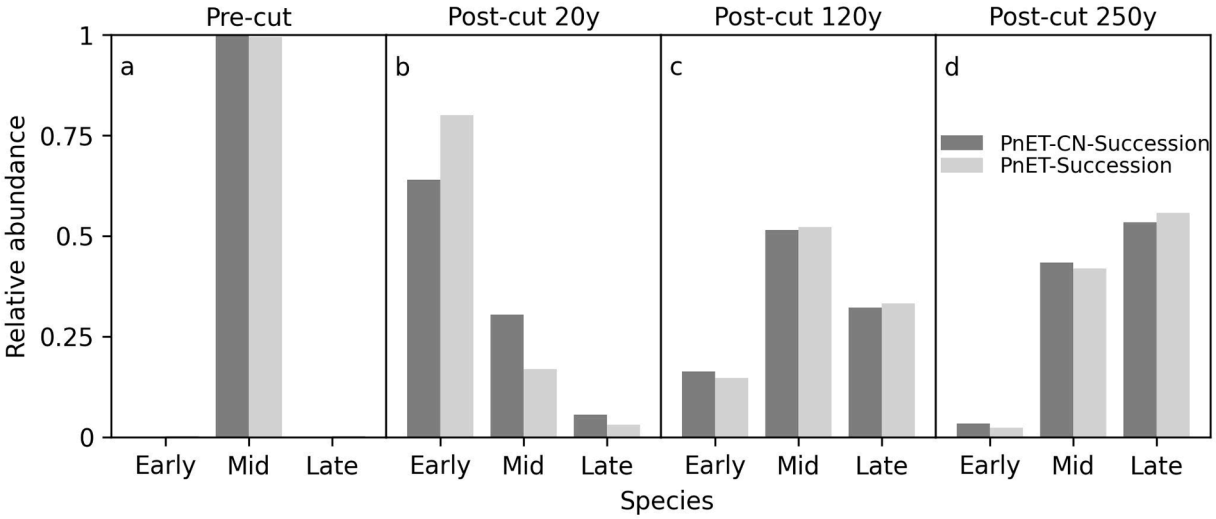

Fig. 7. Dynamics of forest composition in the 100 % harvesting scenario. Harvesting was prescribed in the year 2020. The species relative abundance denotes the biomass composition of grouped species (early, mid, and late successional species) in the pre-cutting year 2019 (a), 20 years after cutting (b) during early succession stage, 120 years after cutting (c) during mid succession stage, and 250 years after cutting(d) during the late succession stage.

and composition (Fig. 7) through the cascading influence of dynamic foliar N. However, the testing also showed some discrepancies compared to the observations. The revised model underestimated GPP at the EMS site from 2001 to 2013. The high measured annual GPP has been partly attributed to increases in midsummer photosynthetic capacity due to the high light level, peak leaf area index (Urbanski et al., 2007), and water-use efficiency (Keenan et al., 2013; Belmecheri et al., 2014). However, these factors do not fully explain the observed trend. The underlying reason is still elusive as these high levels have not persisted, also for reasons that are not clear. Mostly due to the GPP underestimation at the EMS site, the model also underestimated yearly NEP. In the meanwhile, the underestimated NEP could be also caused by an underestimated soil organic carbon accumulation as our modeled soil carbon turnover didn't include the recalcitrant carbon fractions.

Inorganic N exports to streams generally serve as an indicator of the successional stage of the forest (Vitousek and Reiners, 1975). When N exports are less than N deposition, a forest ecosystem accumulates nutrients and carbon, reflecting a young, growing forest. Alternatively, an N export balanced with N deposition indicates a mature forest. In this study, both deciduous and evergreen forests at HF showed the modeled stream N exports were less than N deposition, indicating growing forests, which corroborated the eddy covariance measurements (Figs. 3 and 4). However, Our model didn't include denitrification, a potential N gaseous loss out of the ecosystem as NO, N_2O, and N_2. Although denitrification has not been identified as a major output in budgets for upland northeastern forests at Harvard Forest (Venterea et al., 2003), studies also demonstrated that denitrification rates could be potentially as high as the N deposition in a similar northern hardwood forest in New England (Wexler et al., 2014). Taking denitrification N loss into account could reduce the stream N exports in the modeling, and thus lessen the discrepancy between the modeled and measured values at Arthur upper pipe gauge (Fig. 4b).

Gaps in our understanding of N cycle mechanisms that aren't included in the model are also involved in species-specific nutrient acquisition strategies in competition and establishment preference for nutrients, which may be worth considering in the future research. Species-specific nutrient acquisition can be associated with differences in mycorrhizal associations (Tedersoo and Bahram, 2019). Ectomycorrhizal (EM) fungi have the ability to access organic soil nutrient sources, while arbuscular mycorrhizal (AM) fungi cannot, and generally access soil inorganic N (Read and Perez-Moreno, 2003). At Harvard Forest, EM trees include eastern hemlock, white pine, balsam fir (*Abies balsamea*), red spruce, red oak, and American beech, black birch, and AM trees include red maple and white ash (*Fraxinus americana*). In this study, cohort competition for soil nitrogen was based on cohort nitrogen demand (Section 2.3) without distinct treatment of the nutrient acquisition strategies among species. There is accumulating evidence that AM and EM dominated forests may respond differently to global change drivers (Phillips et al., 2013). e.g., Dong et al. (2018) reported that AM symbionts exhibited greater plant growth than EM symbionts under elevated CO_2 concentration.

The establishment of new cohorts is simulated in the PnET-Succession model as a two-step process: 1) seed dispersal and 2) establishment. When seeds arrive at a cell, the establishment is determined based on tree species and two environmental factors: the light intensity and water availability at the soil surface (Gustafson et al., 2023). Empirically, bedrock material, soil nutrients (e.g. nitrogen availability), and biotic and abiotic disturbance regimes can also influence regeneration (Leuschner and Rode, 1999; Soto et al., 2017). Catovsky and Bazzaz (2002) found that hemlock seedlings at Harvard Forest showed significant positive survival responses to nitrogen availability, while red maple and white pine regeneration underwent nitrogen-induced declines in survival, implying that mid-successional species (red maple, white pine, and red spruce) can increase in the establishment on nitrogen-depleted soils after harvest removal or abandoned agriculture cultivated lands. Land use history and timber harvesting generally impose a long-lasting legacy on soil nitrogen availability, which then influences forest growth (Ollinger et al., 2002b). The uncertainty of soil nitrogen availability on establishment was difficult to estimate, but it seems worth further investigation in the future.

5. Conclusions

The addition of coupled C and N cycling in PnET-CN-Succession added a dynamic to the cohort foliar N variable, which is an essential driver of forest growth. Deciduous and coniferous forests with the N constraint demonstrated distinct C and N cycling patterns in this study that were consistent with empirical observations: faster C and N cycling in deciduous forests, while tighter C and N coupling in coniferous forests. PnET-CN-Succession provides a valuable modeling tool to study interactions between N cycling and succession in the context of disturbances (including forest management) to address changes in forest health, structure, functioning, and services, in terms of biomass, species composition, canopy chemistry, and stream N loss.

CRediT authorship contribution statement

Zaixing Zhou: Writing – review & editing, Writing – original draft, Visualization, Validation, Software, Methodology, Data curation, Conceptualization. **Eric J. Gustafson:** Writing – review & editing, Writing – original draft, Methodology, Conceptualization. **Scott V. Ollinger:** Writing – review & editing, Methodology, Conceptualization. **Andrew P. Ouimette:** Writing – review & editing, Methodology, Conceptualization. **Brian R. Miranda:** Writing – review & editing, Validation, Software, Methodology, Conceptualization. **Matthew J. Duveneck:** Writing – review & editing, Methodology, Data curation, Conceptualization. **Jane R. Foster:** Writing – review & editing, Methodology, Conceptualization. **Brian R. Sturtevant:** Writing – review & editing, Methodology, Conceptualization. **Dustin R. Bronson:** Writing – review & editing, Methodology, Conceptualization. **Danelle Laflower:** Writing – review & editing, Conceptualization.

Declaration of competing interest

The authors declare that they have no known competing financial interests or personal relationships that could have appeared to influence the work reported in this paper.

Acknowledgments

This work was supported by the USDA Forest Service (award numbers 24-JV-11242313-049, 23-DG-11242311-020), the U.S. National Science Foundation (award numbers 1920908, 1637685, and 1832210), and the NH Agricultural Experiment Station (Hatch project NH00711). We thank Matthew Vadeboncoeur for his thoughtful and supportive friend review. Special thanks go to the Harvard Forest LTER for providing field data. The findings and conclusions are those of the authors and should not be construed to represent any official USDA or U. S. Government determination or policy.

Appendices

Forest dynamics with 60 % and 30 % harvesting scenarios

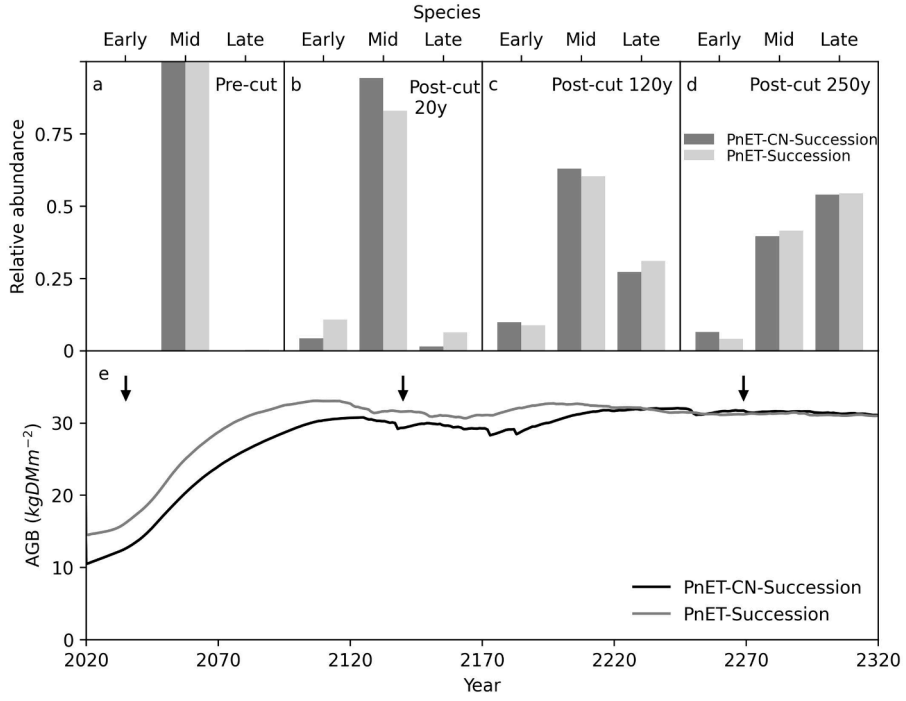

Fig. A1. Dynamics of site above-ground biomass (AGB) and forest composition in the 60 % harvesting scenario. Harvesting was prescribed in the year 2020. The species relative abundance shows the biomass composition of grouped species (early, mid, and late successional species) in the pre-cutting year 2019 (a), 20 years after cutting (b) during early succession stage, 120 years after cutting (c) during mid succession stage, 250 years after cutting(d) during late succession stage. The down arrows, respectively, mark the early, mid, and late succession stages along the dynamics of AGB (e) after harvesting.

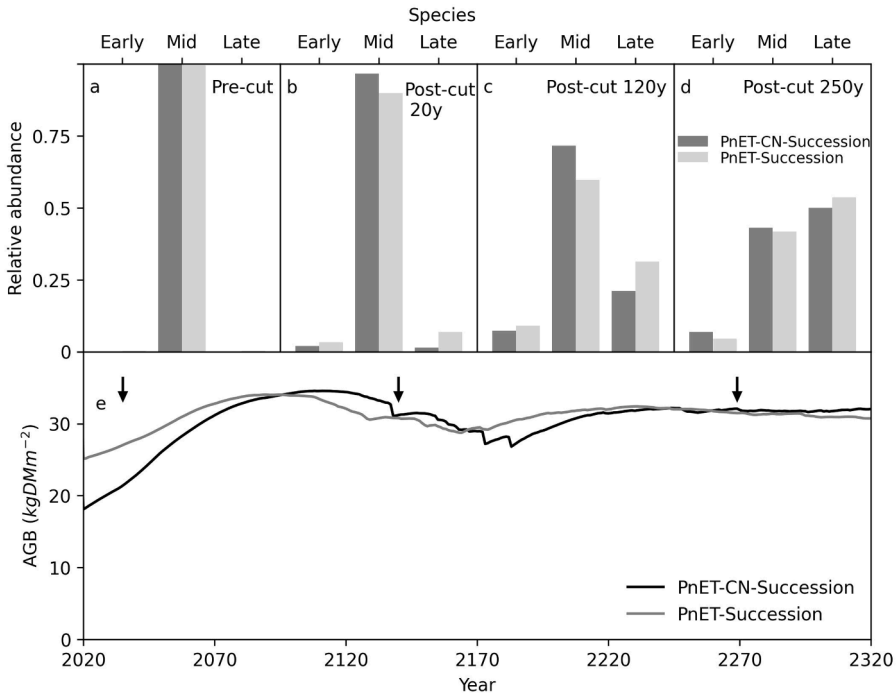

Fig. A2. Dynamics of site above-ground biomass (AGB) and forest composition in the 30 % harvesting scenario. Harvesting was prescribed in the year 2020. The species relative abundance shows the biomass composition of grouped species (early, mid, and late successional species) in the pre-cutting year 2019 (a), 20 years after cutting (b) during early succession stage, 120 years after cutting (c) during mid succession stage, 250 years after cutting(d) during late succession stage. The down arrows, respectively, mark the early, mid, and late succession stages along the dynamics of AGB (e) after harvesting.

Data availability

Data will be made available on request.

References

Aber, J., Federer, C., 1992. A generalized, lumped-parameter model of photosynthesis, evapotranspiration and net primary production in temperate and boreal forest ecosystems. Oecologia 92, 463–474. https://doi.org/10.1007/BF00317837.

Aber, J.D., Driscoll, C.T., 1997. Effects of land use, climate variation, and N deposition on N cycling and C storage in northern hardwood forests. Global. Biogeochem. Cycles. 11, 639–648. https://doi.org/10.1029/97GB01366.

Aber, J.D., Ollinger, S.V., Driscoll, C.T., 1997. Modeling nitrogen saturation in forest ecosystems in response to land use and atmospheric deposition. Ecol. Modell. 101, 61–78. https://doi.org/10.1016/S0304-3800(97)01953-4.

Aber, J.D., Ollinger, S.V., Federer, C.A., Reich, P.B., Goulden, M.L., Kicklighter, D.W., Melillo, J.M., Lathrop, R.G., 1995. Predicting the effects of climate change on water yield and forest production in the northeastern United States. Clim. Res. 5, 207–222. https://doi.org/10.3354/cr005207.

Augusto, L., De Schrijver, A., Vesterdal, L., Smolander, A., Prescott, C., Ranger, J., 2015. Influences of evergreen gymnosperm and deciduous angiosperm tree species on the functioning of temperate and boreal forests. Biol. Rev. 90, 444–466. https://doi.org/10.1111/brv.12119.

Barford, C.C., Wofsy, S.C., Goulden, M.L., Munger, J.W., Pyle, E.H., Urbanski, S.P., Hutyra, L., Saleska, S.R., Fitzjarrald, D., Moore, K., 2001. Factors controlling long- and short-term sequestration of atmospheric CO $_2$ in a mid-latitude forest. Science (1979) 294, 1688–1691. https://doi.org/10.1126/science.1062962.

Belmecheri, S., Maxwell, R.S., Taylor, A.H., Davis, K.J., Freeman, K.H., Munger, W.J., 2014. Tree-ring δ 13 C tracks flux tower ecosystem productivity estimates in a NE temperate forest. Environ. Res. Lett. 9, 074011. https://doi.org/10.1088/1748-9326/9/7/074011.

Bobbink, R., Hicks, K., Galloway, J., Spranger, T., Alkemade, R., Ashmore, M., Bustamante, M., Cinderby, S., Davidson, E., Dentener, F., Emmett, B., Erisman, JW., Fenn, M., Gilliam, F., Nordin, A., Pardo, L., De Vries, W., 2010. Global assessment of nitrogen deposition effects on terrestrial plant diversity: a synthesis. Ecol. Appl. 20, 30–59. https://doi.org/10.1890/08-1140.1.

Catovsky, S., Bazzaz, F.A., 2002. Nitrogen availability influences regeneration of temperate tree species in the understory seedling bank. Ecol. Appl. 12, 1056–1070. https://doi.org/10.1890/1051-0761(2002)012[1056:NAIROT]2.0.CO;2.

Cessna, J.F., Nielsen, C., 2012. Influences of Hemlock woolly adelgid–Induced stand-level mortality on nitrogen cycling and stream water nitrogen concentrations in southern Pennsylvania. cast 77, 127–135. https://doi.org/10.2179/11-025.

Crowley, K.F., Lovett, G.M., Arthur, M.A., Weathers, K.C., 2016. Long-term effects of pest-induced tree species change on carbon and nitrogen cycling in northeastern U.S. forests: a modeling analysis. For. Ecol. Manage 372, 269–290. https://doi.org/10.1016/j.foreco.2016.03.045.

de Bruijn, A., Gustafson, E.J., Sturtevant, B.R., Foster, J.R., Miranda, B.R., Lichti, N.I., Jacobs, D.F., 2014. Toward more robust projections of forest landscape dynamics under novel environmental conditions: embedding PnET within LANDIS-II. Ecol. Modell. 287, 44–57. https://doi.org/10.1016/j.ecolmodel.2014.05.004.

Dong, Y., Wang, Z., Sun, H., Yang, W., Xu, H., 2018. The response patterns of arbuscular mycorrhizal and ectomycorrhizal symbionts under elevated CO2: a meta-analysis. Front. Microbiol. 9, 1248. https://doi.org/10.3389/fmicb.2018.01248.

Duveneck, M.J., Thompson, J.R., Gustafson, E.J., Liang, Y., de Bruijn, A.M.G., 2017. Recovery dynamics and climate change effects to future New England forests. Landscape Ecol. 32, 1385–1397. https://doi.org/10.1007/s10980-016-0415-5.

Dybzinski, R., Farrior, C.E., Ollinger, S., Pacala, S.W., 2013. Interspecific vs intraspecific patterns in leaf nitrogen of forest trees across nitrogen availability gradients. New. Phytol. 200, 112–121. https://doi.org/10.1111/nph.12353.

Ellison, A.M., Orwig, D.A., Fitzpatrick, M.C., Preisser, E.L., 2018. The past, present, and future of the Hemlock Woolly Adelgid (Adelges tsugae) and its ecological interactions with Eastern Hemlock (Tsuga canadensis) forests. Insects. 9, 172. https://doi.org/10.3390/insects9040172.

Finzi, A.C., Giasson, MA., Barker Plotkin, A.A., Aber, J.D., Boose, E.R., Davidson, E.A., Dietze, M.C., Ellison, A.M., Frey, S.D., Goldman, E., Keenan, T.F., Melillo, J.M., Munger, J.W., Nadelhoffer, K.J., Ollinger, S.V., Orwig, D.A., Pederson, N., Richardson, A.D., Savage, K., Tang, J., Thompson, J.R., Williams, C.A., Wofsy, S.C., Zhou, Z., Foster, D.R., 2020. Carbon budget of the harvard forest long-term ecological research site: pattern, process, and response to global change. Ecol. Monogr. 90, e01423. https://doi.org/10.1002/ecm.1423.

Ford, C.R., Elliott, K.J., Clinton, B.D., Kloeppel, B.D., Vose, J.M., 2012. Forest dynamics following eastern hemlock mortality in the southern Appalachians. Oikos. 121, 523–536. https://doi.org/10.1111/j.1600-0706.2011.19622.x.

Foster, D., Barker Plotkin, A., 2023. Hemlock Mapped Tree Plot at Harvard Forest Since 1990. Harvard Forest Data Archive: HF031 (v.25). Environmental Data Initiative. https://doi.org/10.6073/pasta/354ae980bb525f356ffe39073ecc584d.

Foster, D.R., 1992. Land-use history (1730-1990) and vegetation dynamics in Central New England, USA. Journal of Ecology 80, 753–771. https://doi.org/10.2307/2260864.

Fulweiler, R., Orwig, D., 2024. Inorganic Nutrient Concentrations in Forested Headwater Streams at Harvard Forest Since 2017. Harvard Forest Data Archive: HF429 (v.5). Environmental Data Initiative. https://doi.org/10.6073/pasta/ef6bf2d7414ebb6687b2318426d9edcb.

Galloway, J.N., Dentener, F.J., Capone, D.G., Boyer, E.W., Howarth, R.W., Seitzinger, S. P., Asner, G.P., Cleveland, C.C., Green, P.A., Holland, E.A., Karl, D.M., Michaels, A. F., Porter, J.H., Townsend, A.R., Vöosmarty, C.J., 2004. Nitrogen cycles: past,

present, and future. Biogeochemistry. 70, 153–226. https://doi.org/10.1007/s10533-004-0370-0.
Goodale, C.L., Aber, J.D., 2001. The long-term effects of land-use history on nitrogen cycling in Northern hardwood forests. Ecol. Appl. 11, 253–267. https://doi.org/10.2307/3061071.
Groffman, P.M., Driscoll, C.T., Durán, J., Campbell, J.L., Christenson, L.M., Fahey, T.J., Fisk, M.C., Fuss, C., Likens, G.E., Lovett, G., Rustad, L., Templer, P.H., 2018. Nitrogen oligotrophication in northern hardwood forests. Biogeochemistry. 141, 523–539. https://doi.org/10.1007/s10533-018-0445-y.
Gustafson, E., Miranda, B., Sturtevant, B., Zhou, Z., 2023. PnET-Succession v 5.1: Comprehensive description of an Ecophysiological Succession Extension Within the LANDIS-II Forest Landscape Model. The LANDIS-II Foundation.
Gustafson, E.J., 2013. When relationships estimated in the past cannot be used to predict the future: using mechanistic models to predict landscape ecological dynamics in a changing world. Landscape Ecol 28, 1429–1437. https://doi.org/10.1007/s10980-013-9927-4.
Gustafson, E.J., Miranda, B.R., Dreaden, T.J., Pinchot, C.C., Jacobs, D.F., 2022. Beyond blight: phytophthora root rot under climate change limits populations of reintroduced American chestnut. Ecosphere 13, e3917. https://doi.org/10.1002/ecs2.3917.
Gustafson, E.J., Miranda, B.R., Sturtevant, B.R., 2020. How do forest landscapes respond to elevated CO2 and ozone? Scaling Aspen-FACE plot-scale experimental results. Ecosphere 11, e03162. https://doi.org/10.1002/ecs2.3162.
Gustafson, E.J., Sturtevant, B.R., Miranda, B.R., Duveneck, M.J., 2024. Overcoming conceptual hurdles to accurately represent trees as cohorts in forest landscape models. Ecol. Modell. 490, 110657. https://doi.org/10.1016/j.ecolmodel.2024.110657.
Hadley, J.L., Schedlbauer, J.L., 2002. Carbon exchange of an old-growth eastern hemlock (Tsuga canadensis) forest in central New England. Tree Physiol. 22, 1079–1092. https://doi.org/10.1093/treephys/22.15-16.1079.
Huston, M.A., 1991. Use of individual-based forest succession models to link physiological whole-tree models to landscape-scale ecosystem models. Tree Physiol. 9, 293–306. https://doi.org/10.1093/treephys/9.1-2.293.
Jenkins, J.C., Aber, J.D., Canham, C.D., 1999. Hemlock woolly adelgid impacts on community structure and N cycling rates in eastern hemlock forests. Can. J. For. Res. 29, 630–645. https://doi.org/10.1139/x99-034.
Keenan, T.F., Hollinger, D.Y., Bohrer, G., Dragoni, D., Munger, J.W., Schmid, H.P., Richardson, A.D., 2013. Increase in forest water-use efficiency as atmospheric carbon dioxide concentrations rise. Nature 499, 324–327. https://doi.org/10.1038/nature12291.
Larocque, G., Shugart, H., Xi, W., Holm, J., 2016. Forest succession models.
Leak, W.B., 1991. Secondary forest succession in New Hampshire, USA. For. Ecol. Manage 43, 69–86. https://doi.org/10.1016/0378-1127(91)90077-9.
Leuschner, C., Rode, M.W., 1999. The role of plant resources in forest succession: changes in radiation, water and nutrient fluxes, and plant productivity over a 300-yr-long chronosequence in NW-Germany. Perspect. Plant Ecol. Evol. Syst. 2, 103–147. https://doi.org/10.1078/1433-8319-00067.
Lovett, G.M., Goodale, C.L., Ollinger, S.V., Fuss, C.B., Ouimette, A.P., Likens, G.E., 2018. Nutrient retention during ecosystem succession: a revised conceptual model. Front. Ecol. Environ. 16, 532–538. https://doi.org/10.1002/fee.1949.
Mason, R.E., Craine, J.M., Lany, N.K., Jonard, M., Ollinger, S.V., Groffman, P.M., Fulweiler, R.W., Angerer, J., Read, Q.D., Reich, P.B., Templer, P.H., Elmore, A.J., 2022. Evidence, causes, and consequences of declining nitrogen availability in terrestrial ecosystems. Science (1979) 376, eabh3767. https://doi.org/10.1126/science.abh3767.
Mladenoff, D.J., 2004. LANDIS and forest landscape models. Ecological modelling, modelling disturbance and succession in forest landscapes using LANDIS 180, 7–19. https://doi.org/10.1016/j.ecolmodel.2004.03.016.
Munger, M., Wofsy, W., 2024a. Canopy-Atmosphere Exchange of Carbon, Water and Energy at Harvard Forest EMS Tower since 1991. Harvard Forest Data Archive: HF004 (v.36). Environmental Data Initiative. https://doi.org/10.6073/pasta/56c6fe02a07e8a8aaff44a43a9d9a6a5.
Munger, M., Wofsy, W., 2024b. Biomass Inventories at Harvard Forest EMS Tower since 1993. Harvard Forest Data Archive: HF069 (v.42). Environmental Data Initiative. https://doi.org/10.6073/pasta/0292c5bdb53f80dffee596295cb080ca.
Ollinger, S.V., 2003. Forest ecosystems. encyclopedia of life sciences. https://doi.org/10.1038/npg.els.0003190.
NADP, 2019. National Atmospheric Deposition Program Data and Maps. https://nadp.slh.wisc.edu/data.
Ollinger, Scott V., Aber, J.D., Reich, P.B., Freuder, R.J., 2002a. Interactive effects of nitrogen deposition, tropospheric ozone, elevated CO2 and land use history on the carbon dynamics of northern hardwood forests. Glob. Chang. Biol. 8, 545–562. https://doi.org/10.1046/j.1365-2486.2002.00482.x.
Ollinger, S.V., Richardson, A.D., Martin, M.E., Hollinger, D.Y., Frolking, S.E., Reich, P.B., Plourde, L.C., Katul, G.G., Munger, J.W., Oren, R., Smith, ML., U, K.T.P., Bolstad, P. V., Cook, B.D., Day, M.C., Martin, T.A., Monson, R.K., Schmid, H.P., 2008. Canopy nitrogen, carbon assimilation, and albedo in temperate and boreal forests: functional relations and potential climate feedbacks. PNAS 105, 19336–19341. https://doi.org/10.1073/pnas.0810021105.
Ollinger, S.V., Smith, ML., 2005. Net primary production and canopy nitrogen in a temperate forest landscape: an analysis using imaging spectroscopy, modeling and field data. Ecosystems. 8, 760–778. https://doi.org/10.1007/s10021-005-0079-5.
Ollinger, S.V., Smith, M.L., Martin, M.E., Hallett, R.A., Goodale, C.L., Aber, J.D., 2002b. Regional variation in foliar chemistry and n cycling among forests of diverse history and composition. Ecology. 83, 339–355. https://doi.org/10.1890/0012-9658(2002)083[0339:RVIFCA]2.0.CO;2.
Orwig, D., Hadley, J., 2024. Leaf Area Index At Harvard Forest HEM and LPH Towers since 1998. Harvard Forest Data Archive: HF150 (v.27). Environmental Data Initiative. https://doi.org/10.6073/pasta/5f331c9ec6901255aca1d2e04ebd7098.
Orwig, D.A., Plotkin, A.A.B., Davidson, E.A., Lux, H., Savage, K.E., Ellison, A.M., 2013. Foundation species loss affects vegetation structure more than ecosystem function in a northeastern USA forest. PeerJ. 1, e41. https://doi.org/10.7717/peerj.41.
Payne, C.J., Peet, R.K., 2023. Revisiting the model system for forest succession: eighty years of resampling Piedmont forests reveals need for an improved suite of indicators of successional change. Ecol. Indic. 154, 110679. https://doi.org/10.1016/j.ecolind.2023.110679.
Penuelas, J., Fernández-Martínez, M., Vallicrosa, H., Maspons, J., Zuccarini, P., Carnicer, J., Sanders, T.G.M., Krüger, I., Obersteiner, M., Janssens, I.A., Ciais, P., Sardans, J., 2020. Increasing atmospheric CO2 concentrations correlate with declining nutritional status of European forests. Commun. Biol. 3, 1–11. https://doi.org/10.1038/s42003-020-0839-y.
Phillips, R.P., Brzostek, E., Midgley, M.G., 2013. The mycorrhizal-associated nutrient economy: a new framework for predicting carbon–nutrient couplings in temperate forests. New Phytologist 199, 41–51. https://doi.org/10.1111/nph.12221.
Read, D.J., Perez-Moreno, J., 2003. Mycorrhizas and nutrient cycling in ecosystems – a journey towards relevance? New Phytologist 157, 475–492. https://doi.org/10.1046/j.1469-8137.2003.00704.x.
Scheller, R.M., 2018. The challenges of forest modeling given climate change. Landscape Ecol 33, 1481–1488. https://doi.org/10.1007/s10980-018-0689-x.
Scheller, R.M., Domingo, J.B., Sturtevant, B.R., Williams, J.S., Rudy, A., Gustafson, E.J., Mladenoff, D.J., 2007. Design, development, and application of LANDIS-II, a spatial landscape simulation model with flexible temporal and spatial resolution. Ecol. Modell. 201, 409–419. https://doi.org/10.1016/j.ecolmodel.2006.10.009.
Scheller, R.M., Hua, D., Bolstad, P.V., Birdsey, R.A., Mladenoff, D.J., 2011. The effects of forest harvest intensity in combination with wind disturbance on carbon dynamics in Lake States Mesic Forests. Ecol. Modell. 222, 144–153. https://doi.org/10.1016/j.ecolmodel.2010.09.009.
Scheller, R.M., Mladenoff, D.J., 2004. A forest growth and biomass module for a landscape simulation model, LANDIS: design, validation, and application. Ecological modelling, modelling disturbance and succession in forest landscapes using LANDIS 180, 211–229. https://doi.org/10.1016/j.ecolmodel.2004.01.022.
Soto, D.P., Jacobs, D.F., Salas, C., Donoso, P.J., Fuentes, C., Puettmann, K.J., 2017. Light and nitrogen interact to influence regeneration in old-growth *Nothofagus*-dominated forests in south-central Chile. For. Ecol. Manage 384, 303–313. https://doi.org/10.1016/j.foreco.2016.11.016.
Sturtevant, B.R., Gustafson, E.J., He, H.S., 2004. Modeling disturbance and succession in forest landscapes using LANDIS: introduction. Ecological modelling, modelling disturbance and succession in forest landscapes using LANDIS 180, 1–5. https://doi.org/10.1016/j.ecolmodel.2004.07.001.
Tedersoo, L., Bahram, M., 2019. Mycorrhizal types differ in ecophysiology and alter plant nutrition and soil processes. Biol. Rev. 94, 1857–1880. https://doi.org/10.1111/brv.12538.
Uchytil, R.J., 1991. Fire Effects Information System, [Online]. U.S. Department of Agriculture, Forest Service, Rocky Mountain Research Station, Fire Sciences Laboratory (Producer).
Urbanski, S., Barford, C., Wofsy, S., Kucharik, C., Pyle, E., Budney, J., McKain, K., Fitzjarrald, D., Czikowsky, M., Munger, J.W., 2007. Factors controlling CO2 exchange on timescales from hourly to decadal at Harvard Forest. J. Geophys. Res. 112, G02020. https://doi.org/10.1029/2006JG000293.
Venterea, R.T., Groffman, P.M., Verchot, L.V., Magill, A.H., Aber, J.D., Steudler, P.A., 2003. Nitrogen oxide gas emissions from temperate forest soils receiving long-term nitrogen inputs. Glob. Chang. Biol. 9, 346–357. https://doi.org/10.1046/j.1365-2486.2003.00591.x.
Vitousek, P.M., Matson, P.A., Van Cleve, K., 1989. Nitrogen availability and nitrification during succession: primary, secondary, and old-field seres. Plant Soil. 115, 229–239. https://doi.org/10.1007/BF02202591.
Vitousek, P.M., Reiners, W.A., 1975. Ecosystem succession and nutrient retention: a hypothesis. Bioscience 25, 376–381. https://doi.org/10.2307/1297148.
Wexler, S.K., Goodale, C.L., McGuire, K.J., Bailey, S.W., Groffman, P.M., 2014. Isotopic signals of summer denitrification in a northern hardwood forested catchment. PNAS, 201404321. https://doi.org/10.1073/pnas.1404321111.
Wright, I.J., Reich, P.B., Westoby, M., Ackerly, D.D., Baruch, Z., Bongers, F., Cavender-Bares, J., Chapin, T., Cornelissen, J.H.C., Diemer, M., Flexas, J., Garnier, E., Groom, P.K., Gulias, J., Hikosaka, K., Lamont, B.B., Lee, T., Lee, W., Lusk, C., Midgley, J.J., Navas, M.L., Niinemets, Ü., Oleksyn, J., Osada, N., Poorter, H., Poot, P., Prior, L., Pyankov, V.I., Roumet, C., Thomas, S.C., Tjoelker, M.G., Veneklaas, E.J., Villar, R., 2004. The worldwide leaf economics spectrum. Nature 428, 821–827. https://doi.org/10.1038/nature02403.
Xu, C., Gertner, G.Z., Scheller, R.M., 2009. Uncertainties in the response of a forest landscape to global climatic change. Glob. Chang. Biol. 15, 116–131. https://doi.org/10.1111/j.1365-2486.2008.01705.x.
Zhou, Z., Ollinger, S.V., Lepine, L., 2018. Landscape variation in canopy nitrogen and carbon assimilation in a temperate mixed forest. Oecologia 1–12. https://doi.org/10.1007/s00442-018-4223-2.